Applied Catalysis A, General 661 (2023) 119260

Contents lists available at ScienceDirect

Applied Catalysis A, General

journal homepage: www.elsevier.com/locate/apcata

Spectroscopic insights into the role of CO_2 on the nature of Cr species in a CrO_X/Al_2O_3 catalysts during ethane dehydrogenation with CO_2

Gustavo do N. Franceschini [a,b], Patricia Concepción [a,*], Marcio Schwaab [b], Maria do Carmo Rangel [c], Joaquín Martínez-Triguero [a], José M. López Nieto [a,*]

[a] Instituto de Tecnología Química, Universitat Politècnica de València, Consejo Superior de Investigaciones Científicas, 46022 Valencia, Spain
[b] Escola de Engenharia, Universidade Federal do Rio Grande do Sul, Porto Alegre, RS, Brazil
[c] Institut de Quimico de Química, Universidade Federal do Rio Grande do Sul, Porto Alegre, RS, Brazil

ARTICLE INFO

Key words:
CrOx-based Catalysts
Ethane dehydrogenation
Carbon dioxide, ethylene
In situ Raman

ABSTRACT

The dehydrogenation of ethane with CO_2 was studied on $CrOx/Al_2O_3$ catalysts (8 wt% of CrO_x) in the 600–675 °C temperature range. The role of CO_2 was determined by comparison with catalytic and spectroscopic data of ethane dehydrogenation without CO_2. Characterization of fresh catalyst suggested an intimate interaction of Cr and support. Moreover, in situ Raman spectroscopic analysis combined with XPS studies done on reaction exposed samples indicated changes in both the nature of active Cr species and the reaction mechanism depending on the reaction conditions (i.e., presence/absence of CO_2, and the reaction temperature). At lower temperatures (600–625 °C), CO_2 promotes the re-oxidation of Cr^{3+} to Cr^{6+} favoring the oxidative dehydrogenation (ODH) route. While at higher temperatures (650–675 °C), the reaction occurs mainly via a catalytic dehydrogenation mechanism, as CO_2 is no longer capable of re-oxidizing Cr^{3+} to Cr^{6+}, with CO_2 inhibiting partially the formation of coke.

1. Introduction

Ethylene is the most important feedstock in Petrochemistry, and due to high consumption in many applications, the global ethylene capacity has increased in the last decade, and it is expected to reach more than 200 million tons by 2026 [1]. Ethylene is produced almost exclusively in the chemical sector by steam cracking [2], a high energy consuming and non-catalytic process [3,4]. Additional disadvantages include low yield of ethylene and high amount of coke production [5,6]. In this scenario, the development of alternative and cost-effective processes to produce olefins is highly desirable [5–8].

The selective oxidative dehydrogenation of ethane (ODHE) has been proposed as a promising alternative route to ethylene [8–16], exploiting cheap ethane (from both natural or shale gas), due to the exothermic character of the reaction, the in-situ reactivation of the catalysts and the relatively low reaction temperatures required. Although the main studies on ethane ODHE have been carried out using oxygen/air as oxidant [8–11], the number of studies on ethane ODH, in which CO_2 is used as a soft oxidant (ODHE-CO_2), has grown in the last years [12–16]. This is so because the use of CO_2 as oxidant could favor the formation of ethylene with net negative CO_2 emissions, even more so if the ODHE-CO_2 reaction is complemented with a certain contribution of dry reforming to obtain ethylene and synthesis gas [15,16].

Despite the common interest on using O_2 as oxidant in ODHE, some drawbacks include its excessive oxidative power, leading to the oxidation of the desired products, and their flammability, that requires additional safety precautions. Moreover, the reaction with oxygen is exothermic, requiring ways to remove the generated heat [13]. In contrast, there are several potential ways for the development of alternative technologies utilizing CO_2 as a soft oxidant and promoter to produce chemical [15,16]. CO_2 is a mild oxidant, thus making reoxidation of the active centers slower when compared to the reoxidation caused by oxygen, while also capable of partially removing coke by the reverse Boudouard reaction, or promoting other reactions [15]. However, the ODHE-CO_2 is a thermodynamically un-favored process, competing at the reaction temperatures of 600–700 °C with ethane dry reforming and ethane/ethylene decomposition reactions, the last ones with almost 100% conversion [15]. Thus, catalyst development slowing down the undesired reactions is critical for high olefin selectivity.

Over the years, different metallic oxides were used as catalysts for

* Corresponding authors.
E-mail addresses: pconcepc@upvnet.upv.es (P. Concepción), jmlopez@itq.upv.es (J.M. López Nieto).

https://doi.org/10.1016/j.apcata.2023.119260
Received 13 February 2023; Received in revised form 7 May 2023; Accepted 8 May 2023
Available online 10 May 2023

alkane ODH with CO_2 as soft oxidant [12–16], in which chromium-based catalysts seem to show great activity in oxidative reactions [17–27], due to its different oxidation states and its capability of undergoing a redox cycle [21,22]. Chromium oxide is typically supported on materials with high surface areas [17,19–21,24] or incorporated in microporous materials [18,23,26]. For instance, Bugrova et al. [22] studying supported chromium oxide on aluminum, zirconium and cerium oxides, as well as a mixed support of cerium and zirconium, observed that the catalytic activity was extremely dependent on the redox properties of the chromium species. In this sense, the catalysts that presented a higher Cr^{6+}/Cr^{3+} ratio showed the best ethane conversion and ethylene selectivity. Furthermore, the nature of the support also influenced the reactional paths followed during the process. The alumina-based catalyst, for example, presented a CO/C_2H_4 formation rate ratio very close to 1, which indicates that the overall oxidative dehydrogenation reaction is the main reaction. The zirconium-based catalyst, on the other hand, showed similar catalytic activity, but a CO/C_2H_4 ratio close to 2 at high temperatures, indicating the occurrence of parallel reactions.

It is widely accepted that Cr^{6+} species are responsible for the high catalytic activity and ethylene formation of chromium-based catalysts in dehydrogenation reactions [21–26]. XPS studies on chromium oxide supported on the SBA-15, with different pore sizes, showed that the optimum catalyst had the highest Cr^{6+}/Cr^{3+} atomic ratio [24]. Similar results were found on silica-supported chromium catalysts promoted by different oxides, such as Zr, Sr, Sn, and Ce [21].

The spent catalysts presented significant changes in the Cr^{6+}/Cr^{3+} ratios, as the Cr^{6+} species were completely reduced in some cases. At the same time, Cr^{3+} species have been suggested to act as active sites on propane dehydrogenation on zirconium-supported chromium catalysts [27]. In this way, it has been proposed that Cr^{3+} species (that were reduced from Cr^{6+} during reaction) can also function as active sites, while dispersed Cr^{3+} (that were already present on the fresh catalyst) are considered to be less active [28]. This is because the reduced samples can more easily participate in the redox cycle, on contrary to the dispersed samples, which presents a stronger interaction with the support.

It is well known that two types of surface Cr^{6+} species are present in supported chromium oxide catalysts as observed by in situ Raman spectroscopy [29], which were named “monomeric” or “isolated” and “polymeric” species. The first were difficult to be reduced, while the latter were more easily reduced on the same support. These species were later denominated “hard” and “soft”, respectively, by Baek et al. [30]. The soft species presented a low interaction with the support, a mesoporous silica, and showed a greater facility to be reduced to Cr^{3+} and to be re-oxidized to Cr^{6+}, which gave the catalysts with larger quantities of soft species a higher catalytic activity. Consequently, although it is important to obtain a catalyst with a high ratio of Cr^{6+}/Cr^{3+} species, it is also very important that the Cr^{3+} species can be readily oxidized to the original Cr^{6+} oxidation state, in order to keep the redox cycle working, since it is precisely the reoxidation process of Cr^{3+} species that will recover the lattice oxygen species.

In the present study, chromium-based catalysts (8 % mass wt.) supported on γ-alumina were evaluated on the production of ethylene in the presence and absence of CO_2. The experiments were conducted in the temperature range of 600–675 °C. A careful analysis of the ratio of H_2, CO and CH_4 in relation to ethylene was performed, in order to verify the different reactions and pathways most likely to occur between the two routes, likely to occur between the dehydrogenation and oxidative dehydrogenation routes. CO_2 activation and the nature of the chromium active species will be discussed based on in situ spectroscopic studies.

2. Experimental

2.1. Catalyst preparation

Alumina-supported chromium catalysts were prepared by wet impregnation of γ-Al_2O_3 ($S_{BET} = 216\ m^2\ g^{-1}$, from ABCR, 97%) with an aqueous solutions of chromium nitrate $Cr(NO_3)_3{\cdot}9\ H_2O$ (Sigma-Aldrich, 99 %). The chromium loading selected (ca. 8 wt%) corresponds to one theoretical monolayer covering the surface of support (i.e., 5 atoms Cr per nm^2 of the support [22]), in order to maximize the Cr^{6+}/Cr^{3+} ratio. The catalysts were dried overnight at 100 °C and calcined at 650 °C for 4 h (2 °C min^{-1}). The used catalysts will be named as 8CrAl(x)y, with x indicating whether they were tested in the presence of CO_2 or N_2, and y the reaction temperature. For example, the catalyst 8CrAl(CO_2)650 was tested in ethane ODH, in the presence CO_2, at a reaction temperature of 650 °C.

2.2. Catalyst characterization

N_2-adsorption isotherms were recorded in a Micromeritics ASAP 2000 device and the Brunauer-Emmet- Teller (BET) method was used to estimate the surface areas. The solids were degassed in vacuum at 300 °C prior to the analysis.

X-ray diffraction patterns were collected in an Enraf Nonius FR590 diffractometer with a monochromatic CuKα1 source operated at 40 keV and 30 mA.

Raman spectra were obtained in an inVia Renishaw spectrometer, equipped with an Olympus microscope. The laser wavelength was 514 nm, generated with a Renishaw HPNIR laser with a power of approximately 15 mW. In situ Raman studies were done using a commercial Linkam 1000 Raman cell. The reaction has been done in a flow of 30 mL min^{-1} ethane/N_2 (molar ratio 12/88) or ethane/CO_2/N_2 (molar ratio 10/20/70), and the reaction temperature was set to 600 °C or 650 °C with a heating ramp of 10 °C min^{-1}. Once achieved the target temperature, the reaction was kept for 0.5 and 3 h. Spectra were acquired at specific reaction conditions, stopping the reaction, switching from the reactant gases to He flow and cooling down to 200 °C.

UV–visible reflectance spectroscopy (DR-UV–vis) measurements of the solids were carried out using a Varian spectrometer model Cary 5000, within the 200 − 800 nm range.

Temperature-programmed reduction experiments (H_2-TPR) were performed in an Autochem 2910 (Micromeritics) equipped with a TCD detector. The solids were heated until 800 °C, with a heating rate of 10 °C min^{-1} and the reducing gas was composed of 10 % H_2 in Ar, with a total flow rate of 50 mL min^{-1}.

TG-DTA analyses of the spent catalysts were performed in a Mettler-Toledo thermobalance (TGA/SDTA 851). Approximately 10 mg of each solid were introduced in the device and heated up to 600 °C under synthetic air flow (50 mL min^{-1}). The heating rate used was 10 °C min^{-1}.

X-ray photoelectron spectra (XPS) were collected using a SPECS spectrometer equipped with an MCD-9 detector and using a non-monochromatic AlKα (1486.6 eV) X-ray source. Spectra were recorded using an analyzer pass energy of 30 eV, an X-ray power of 100 W and an operating pressure of 10^{-9} mbar. Data processing was performed using the CASA software. Cr_2O_3 (supplied from Sigma-Aldrich) was used as reference for determining multiplet splitting and spectra deconvolution parameters. For the catalytic XPS studies a high-pressure catalytic reactor (HPCR) connected under vacuum to the XPS chamber was used. The reaction was done in a flow of 30 mL min^{-1} ethane/N_2 (molar ratio of 12/88) or ethane/CO_2/N_2 (molar ratio of 10/20/70), and the reaction temperature was set to 600 °C or 650 °C with a heating ramp of 10 °C min^{-1}. Once achieved the target temperature, the reaction was kept for 2 h. In an additional experiment, after ethane/N_2 flow conditions, the reactant feed was switch to 30 mL/min CO_2/N_2 (vol% 40/60) and the temperature increased up to 700 °C at a heating ramp of 10 °C min^{-1}.

TPR-C_2H_6 and TPO-CO_2 experiments were conducted using a quartz micro reactor coupled to a quadrupole mass spectrometer (Omnistar, Balzers). 180 mg catalyst was preactivated in O_2 flow (18 mL min^{-1}) at 300 °C. After pre-activation the sample was cooled down in Ar flow (18 mL min^{-1}) to 25 °C. Once stabilized the temperature, the reactant feed was switched from Ar to 12 mL min^{-1} (Ethane/N_2 molar ratio of 12/88). Reaction temperature was increased up to 600 °C with a heating ramp of 10 °C min^{-1} and the reaction products analyzed by on line MS. After 1 h at 600 °C, the temperature was decreased to 25 °C in Ar flow. Once stabilized the temperature, the gas was switched from Ar to 12 mL min^{-1} (CO_2/N_2 molar ratio of 40/60) and the temperature increased to 700 °C at 10 °C min^{-1}. Again, reaction products were analyzed by MS.

2.3. Catalytic tests

Catalytic tests were carried out under steady state conditions in a fixed bed quartz reactor (i.d. 90 mm, length 400 mm) at temperatures in the range of 600–675 °C and atmospheric pressure. For the ODHE experiments, the feed consisted of an ethane/CO_2/N_2 mixture with 10/20/70 volumetric ratio and total flow rate of 50 mL min^{-1}. Catalyst mass was 400 mg in all experiments, and it was always diluted in silicon carbide, resulting in a contact time (W/F) of 29.9 g_{cat} h mol^{-1}_{ethane}. In the experiments in the absence of CO_2 (catalytic dehydrogenation, CD), the feed consisted of an ethane/N_2 mixture with a 10/90 volumetric ratio, keeping the total flow of 50 mL min^{-1} and 400 mg of catalyst mass. The catalytic performance was evaluated for a 4.2 h reaction. The reactor was heated at 10 °C min^{-1} and during this process the catalyst was put in contact with the gaseous mixture, excluding ethane. When the desired temperature was reached, the system was left on hold for 15 min for stabilization purposes and only then was ethane finally put in contact with the catalyst.

Reactants and products were analyzed by gas chromatography using two packed columns: (i) molecular sieve 5 A (3 m); and (ii) Porapak Q (3 m). Blank experiments were also carried out, and null conversions of ethane were found.

The conversion of reactants (X) and yield (Y) and selectivity (S) of products were calculated by the following equations, where F is the molar flowrate of the components.

$$X_i = \frac{F_i^{in} - F_i^{out}}{F_i^{in}} \text{ i = ethane or } CO_2 \text{ (Eq. 1)}$$

$$Y_i = \frac{F_i^{out}}{F_{ethane}^{in}} \text{ i = ethylene (Eq. 2)}$$

$$Y_j = \frac{F_j^{out}}{F_{CO2}^{in}} \text{ j = CO} \quad \text{Eq. 3)}$$

$$S_i = \frac{F_i^{out}}{F_{ethylene}^{out} + F_{methane}^{out}} \text{ i = ethylene or } methane \text{(Eq. 4)}$$

3. Results and discussion

3.1. Catalytic results

Fig. 1 shows the catalytic results during the ethane ODH with CO_2 (ODHE-CO_2) over a supported chromium oxide catalyst in the 600–675 °C temperature range. Both conversion of ethane (Fig. 1a) and yield to ethylene (Fig. 1c) increase when increasing the reaction temperature. On the other hand, the conversion of CO_2 (Fig. 1b) and the yield of CO (Fig. 1d) were lower to those achieved for ethane conversion and yield of ethylene, respectively. But, since we are using an ethane/CO_2 ratio of 1/2 in the feed, it can be concluded that there is a relatively similar reaction rate for both ethane and CO_2 conversion.

In addition, a catalyst decay has been observed in all temperature range studied, this effect being more important when increasing the reaction temperature. We noticed that the loss of activity observed in the ODH experiments remained similar in all reaction temperatures, close to 50 %.

For comparison, Fig. 2 presents the catalytic results for the catalytic

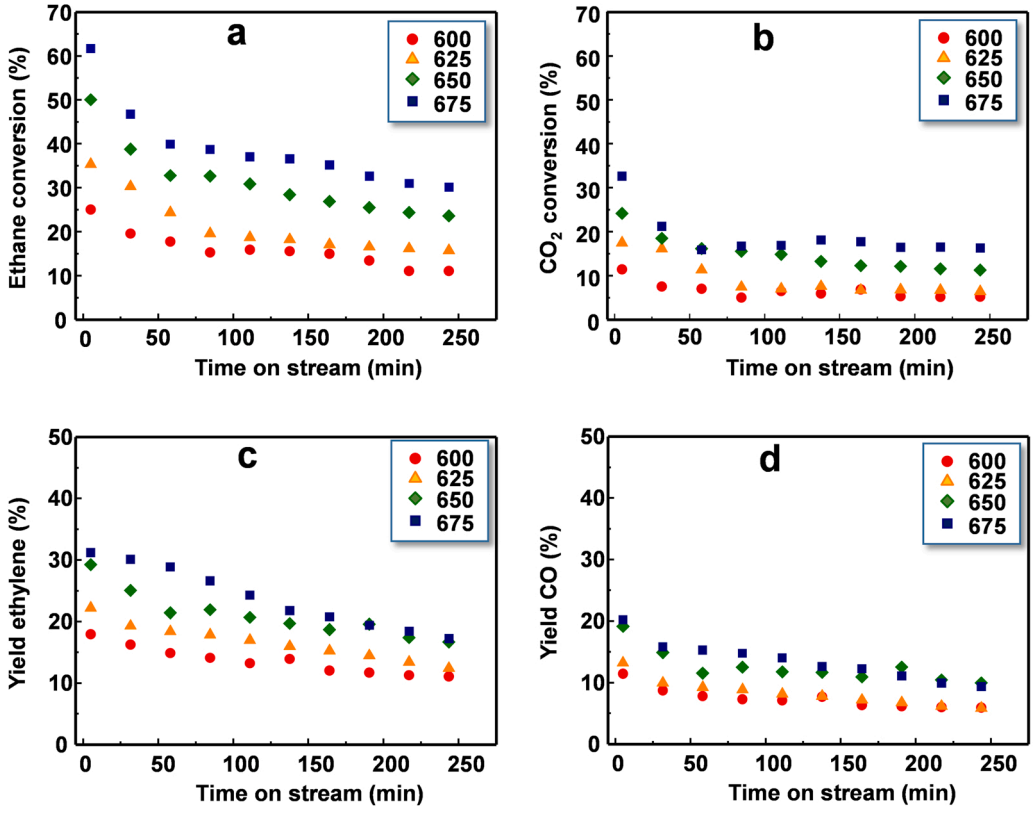

Fig. 1. Variation of conversion of ethane (a), conversion of CO_2 (b), yield of ethylene (c) and yield of CO (d) with time on stream for the ethane conversion in the presence of CO_2, ODHE-CO_2, at a reaction temperature of: 600 °C (●); 625 °C (▲); 650 °C (◆); and 675 °C (■). Reaction conditions in text.

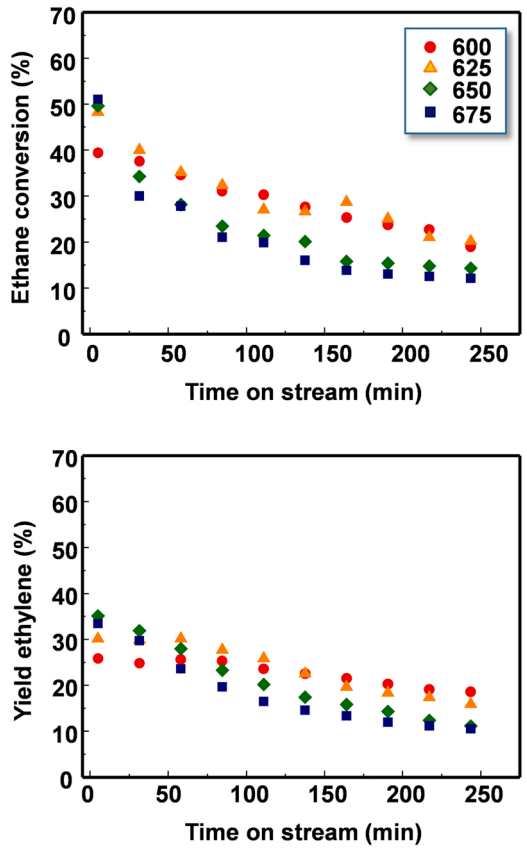

Fig. 2. Variation of conversion of ethane (a) and yield of ethylene (b) with time on stream for the ethane conversion in the absence of CO_2, CD, at a reaction temperature of: 600 °C (●); 625 °C (▲); 650 °C (◆); and 675 °C (■).

ethane transformation in the absence of CO_2 (i.e., catalytic dehydrogenation, CD) in the same reaction temperature range of 600–675 °C. At short time on stream, both ethane conversion and yield of ethylene increase with the reaction temperature. However, at higher time on streams, a catalyst decay is observed. This catalyst decay strongly increases when the reaction temperature is increased.

Fig. 3 shows the variation of selectivity to ethylene and methane during the transformation of ethane in the presence (Fig. 3a) and in the absence (Fig. 3b) of CO_2. In general, the selectivity to ethylene decreases slightly with the reaction temperature, being somewhat lower in the case of experiments in the presence of CO_2, due to the increase in methane formation.

On the other hand, as displayed in Fig. 2, the deactivation rate of the catalyst in the absence of CO_2 increased with the reaction temperature and was even more severe, showing an important loss of activity. Thus, at a time on stream of 250 min, the loss of activity was of ca. 71% (the ethane conversion varies from 49 % to 14%) or 76% (the ethane conversion varies from 51 % to 12 %), for the experiments conducted at 650 and 675 °C, respectively. Furthermore, the initial conversion of ethane at 625–675 °C were practically the same, but the deactivation rate kept increasing. This shows that increasing the temperature in the CD experiments did not improve ethylene yield, contrary to what was observed for the ODHE-CO_2 experiments. A summary of the catalytic results for the experiments in the presence and in the absence of CO_2 is presented on Table S1 (supplementary information).

A comparison between results for ethane conversion in the presence of CO_2 (Fig. 1a) and in absence of CO_2 (Fig. 2a) are shown in Fig. S1a and S1b (supplementary information). A considerable shift in the conversion behavior of ethane can be seen influenced by the presence of CO_2.

Comparing the results at 600 and 625 °C, ethane conversion is higher on the CD experiments throughout the whole experiment, however that completely changes at higher reaction temperatures (i.e., 650 and 675 °C), and from that point onwards the conversion on the ODH experiment was kept higher. The same can be seen on the yield of ethylene obtained: the final yield of ethylene (time on stream of ca. 250 min) at 600 °C in the ODH experiments is practically the same at 675 °C for the CD experiments, whereas the final yield of ethylene at

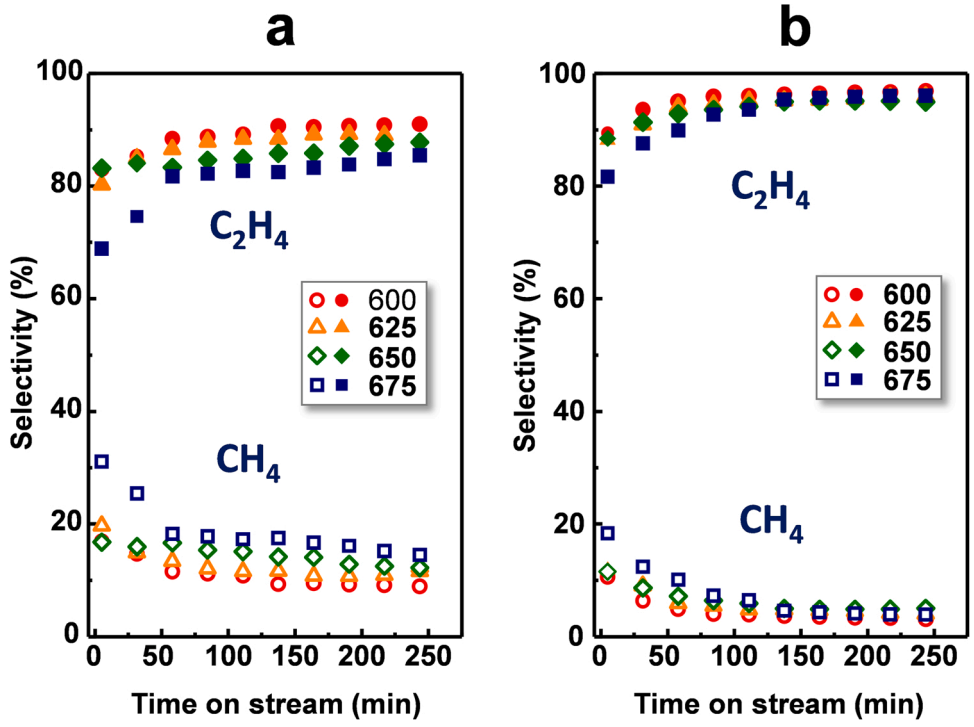

Fig. 3. Variation of the selectivity to ethylene (full symbols) and methane (empty symbols) with time on stream during the transformation of ethane in the presence of CO_2 (a) or in the absence of CO_2 (b). Reaction temperature of: 600 °C, 625 °C, 650 °C or 675 °C. Reaction conditions in text.

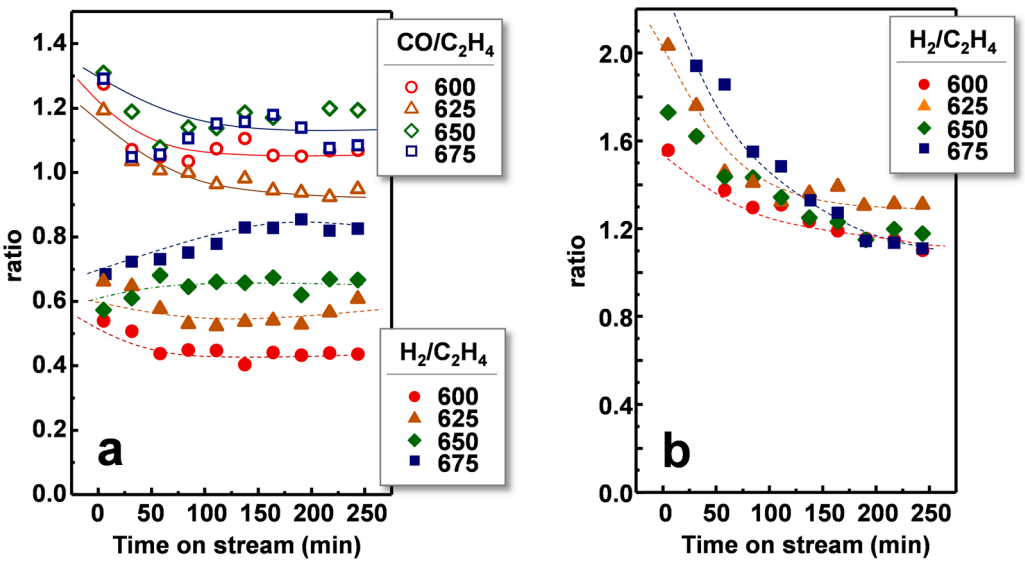

Fig. 4. Variation of the H_2/C_2H_4 and CO/C_2H_4 ratios with time on stream at reaction temperatures of 600, 625, 650 or 675 °C during the ethane transformation in the presence of CO_2 (a), or in the absence of CO_2 (b). The catalytic results were achieved at a time on stream of ca. 250 min. The lines were drawn to help visualization.

675 °C for the ODH experiment is higher than any yield value found on the CD experiments. In addition, the ODH experiments presented a positive tendency in the overall ethylene yield in regard to temperature; that is, as the temperature increased, the reaction yield also increased. The ethylene yield tendency for the CD experiments do not present the same behavior, as the points overlap with each other. When the experiment starts, ethylene yield is higher at 650 and 675 °C. However, this is altered during the experiment, as the yield of ethylene at 600 °C is the highest close to 3 h of reaction time and remains this way until the end of the experiment. Furthermore, the higher the temperature is, the faster the yield diminishes, as the yield of ethylene at 675 °C is already lower than 650 °C at a reaction time of 30 min.

In order to develop hypothesis about the different reactions that are occurring in each experiment, the mole ratio of H_2, CO and CH_4 in relation to ethylene were calculated at different reaction temperatures and at a time on stream of ca. 250 min, in the presence (Fig. 4a) or in the absence (Fig. 4b) of CO_2. Table S2 (Supplementary information) shows a summary of the mole ratio of side products in relation to ethylene reaction times of 137 and 250 min. The ratio found for the ODH experiments remained practically constant during the experiment. The same cannot be said for the CD experiments, since the initial ratio for both H_2 and CH_4 in relation to ethylene were much higher than the ones found at 137 and 250 min.

In the case of ethane ODH with CO_2 (Fig. 4a), it can be seen that side reactions become more predominant as the temperature increases, since in addition to the formation of methane (Fig. 3) the H_2/C_2H_4 increases with the reaction temperature. The CO/C_2H_4 ratio, however, remained somewhat constant, between 0.9 and 1.2. Methane was also identified, possibly related to a non-selective oxidation of ethane in the presence of CO_2 [31]. The methane production remained low throughout the experiment, less than five times the production of ethylene at its maxima, while the H_2 production was higher but remained lower than the production of CO and ethylene overall. This higher production of H_2 might be explained by the increase in the reaction temperature, which favors cracking reactions and the non-oxidative dehydrogenation reaction.

Fig. 4b shows H_2/C_2H_4 ratio during the catalytic dehydrogenation of ethane in absence of CO_2. It can be observed that the H_2/C_2H_4 ratio tends to 1 at high reaction times, which is in accordance with the catalytic dehydrogenation stoichiometry. The results achieved at low time

Table 1
Structural properties of the catalysts.

Catalyst [1]	XPS Data			TG
	$Cr2p_{3/2}$ B.E. (eV)		Atomic composition	Mass loss
	Cr^{3+} (%)	Cr^{6+} (%)	O: C: Cr: Al (%)	(%)
Cr_2O_3	576.4 (100 %)	—	43.5: 40.9: 15.5:0.0	n.d.
8CrAl	576.9 (65.1 %)	580.0 (34.9 %)	47.8: 14.8: 2.5: 34.9	n.d.
8CrAl(N_2)600	576.8 (100 %)	—	36.3: 32.4: 2.4: 28.9	9.1
8CrAl(N_2)650	576.7 (100 %)	—	35.1: 35.8: 2.1: 27.0	10.2
8CrAl(N_2)675	n.d.	n.d.	n.d.	10.6
8CrAl(N_2)600+ CO_2 700 [2]	576.8 (64.8 %)	580.0 (35.2%)	51.7: 2.9: 3.2: 42.2	n.d.
8CrAl(N_2)650+ CO_2 700 [3]	576.7 (83.8 %)	580.5 (16.2%)	44.1: 19.2: 2.4: 34.3	n.d.
8CrAl(CO_2)600	576.4 (89.4 %)	580.1 (10.6%)	33.7: 36.5: 1.9: 27.7	2.8
8CrAl(CO_2)650	576.7 (100 %)	—	32.3: 37.3: 1.7: 28.7	4.7
8CrAl(CO_2)675	n.d.	n.d.	n.d.	6.6

1) Nomenclature of samples as described in experimental section.

2) Sample treated in an ethane/N_2 (molar ratio of 12/88) at 600 °C for 2h and then treated with CO_2/N_2 at 700 °C.

3) Sample treated in an ethane/N_2 (molar ratio of 12/88) at 650 °C for 2h and then treated with CO_2/N_2 at 700 °C.

on stream, with H_2/C_2H_4 ratio of ca. 1.6–2.0, should be related to the yield of hydrogen during the coking reaction.

On the other hand, the absence of CO_2 in the feed resulted in a higher quantity of coke found (see Table 1), due to the thermal cracking of ethane and/or ethylene. The small traces of methane found could be due to a non-selective cracking of ethane, generating methane, hydrogen and coke.

From a direct comparison of both systems, it can be noted that the mole ratio of the main side products - CO in the ODHE-CO_2 experiments and H_2 in the CD experiments - in relation to ethylene is very close to 1 in all cases. This means that the proposed reaction for each case was oxidative dehydrogenation and catalytic dehydrogenation, respectively. Nevertheless, the effects of side reactions were noticeable on all experiments, even more at higher temperatures, in which cracking become more likely to occur.

3.2. Characterization results

The XRD pattern of fresh catalyst is depicted in Fig. 5a. The material shows peaks related to chromium oxide, at $2\theta = 24.5°$, 33.6°, 36.5°, 50.2° and 54.9°, related to Cr_2O_3 (PDF# 38–1479) [20,24,26], and γ-alumina, at $2\theta = 46°$ and 67° [32]. No distinguishable features between the catalysts can be seen, even on the spent ones. The low chromium peak intensity observed suggests crystals of small sizes of chromium oxide particles well dispersed on the surface of the support.

The Raman spectrum of fresh catalyst, presented in Fig. 5b, shows two small bands related to Cr_2O_3 at 344 and 550 cm^{-1} and a higher intensity band related to polymeric CrO_3 species at 860 cm^{-1} [21,23,33,34]. Accordingly, both crystalline Cr_2O_3 and polymeric Cr^{6+}-species are present in the catalyst.

The structural properties of the support and catalyst were determined by nitrogen adsorption. The γ-alumina support had a surface area of 216 $m^2\ g^{-1}$, a pore volume of 0.46 $cm^3\ g^{-1}$ and a pore diameter of 7.6 nm. After chromium impregnation and calcination, there is a small alteration in the structure of the catalyst, presenting a surface area (180 $m^2\ g^{-1}$) and pore volume (0.38 $cm^3\ g^{-1}$) slightly smaller, while the pore diameter (7.9 nm) increases slightly.

DR-UV-Vis results for the fresh catalyst (Fig. 5c) present two intense bands at 260 and 370 nm that represent the Cr^{6+} state for chromium species with tetrahedral structure and one main band at 470 nm that represents octahedral Cr^{3+} [18,21,33,35].

TPR- H_2 pattern of fresh catalyst is presented in Fig. 5d. One major peak can be seen around 295 °C, which corresponds to the reduction of Cr^{6+} to Cr^{3+} [19–26,35–39], in accordance with previous analysis, in which only one reduction state was found. Two minor shoulders can be seen around 450 °C and 550 °C, which could be related to one step reduction of Cr^{6+} species stabilized on the alumina surface and to the reduction of bulk chromate species, respectively [40].

After reaction, the spent catalysts were analyzed by thermogravimetric analyses in the temperature range of 50–750 °C and the results are shown in Table 1. The catalysts that reacted in the absence of CO_2 showed a higher value of coke in its surface, in agreement with characterization results discussed below. Most noticeable, coke deposition during the CD experiments at a reaction temperature 650 °C was higher than the ODH experiments at 675 °C. The loss of catalytic activity at 650 and 675 °C in the absence of CO_2 is practically the same, as are the values for coke deposition.

In order to get a deeper understanding of the nature of Cr species and try to correlate them with the reaction mechanism, XPS studies were done on fresh (Fig. 6a) and spent samples (Fig. 7). For the last case the samples were exposed to reaction conditions in a high-pressure catalytic reactor connected under vacuum to the XPS analyze chamber. After reaction the sample were transferred under vacuum conditions to the XPS analyze chamber. For a clear assessment of oxidation states, Cr_2O_3 was taken as reference and fitted into a main peak and two multiple splitting peaks (details in SI), according to previous works in the literature [41,42]. Taken into account this deconvolution pattern, two oxidation states of Cr can be detected in the fresh sample, i.e., Cr^{6+} with BE 580.0 eV and Cr^{3+} with the main component at 576.9 eV and the two satellites at 578.4 and 580.8 eV, respectively (Fig. 6a). Quantitative analysis point to 34.9% Cr^{6+} and 65.1 % Cr^{3+}. In fact, the coexistence of both oxidation states is in line with the Raman analysis discussed above.

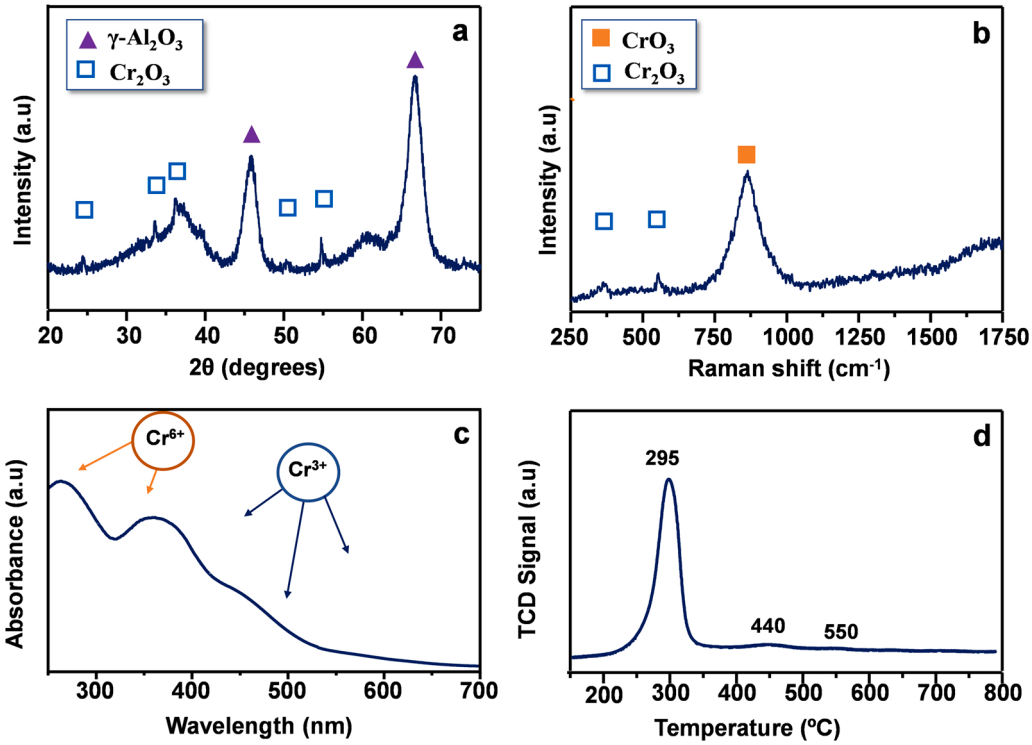

Fig. 5. Characterization results of fresh catalyst (8CrAl sample): (a) XRD pattern; (b) Raman spectrum; (c) DR-UV–vis spectrum; and (d) H_2-TPR pattern.

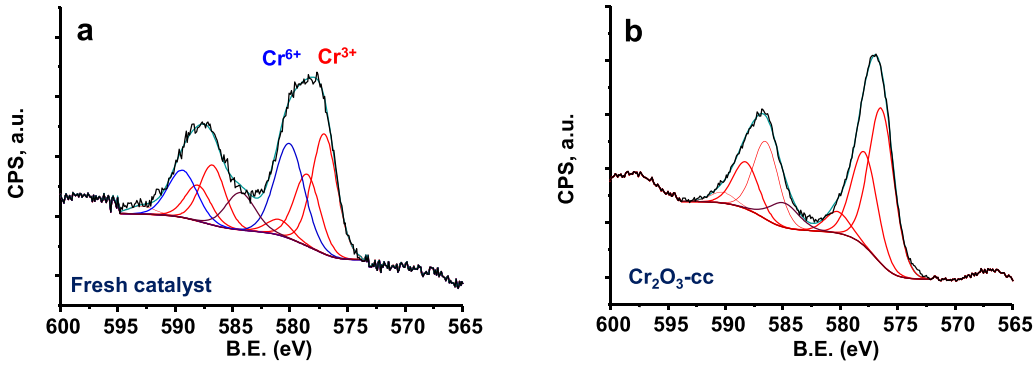

Fig. 6. a) XPS spectrum of the Cr 2p doublet in the fresh catalyst (sample 8CrAl); b) Cr2p spectrum of a commercial Cr_2O_3 sample included as reference (deconvolution details in SI). Red line corresponds to Cr^{3+} (main peak and two multiplet splitting peaks at higher BE); and blue line corresponds to Cr^{6+}.

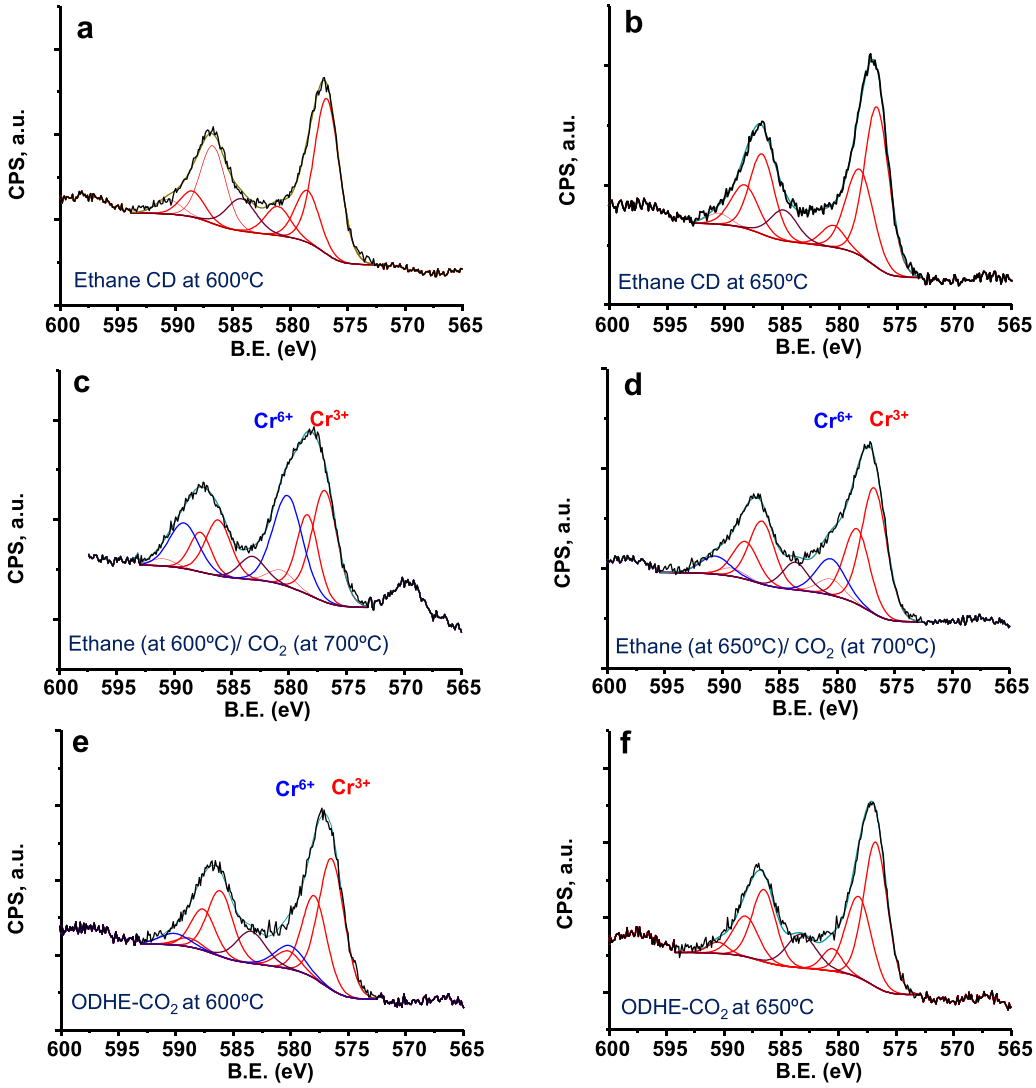

Fig. 7. XPS spectra of the Cr 2p doublet of catalysts. (i) After ethane dehydrogenation conditions, at 600 (a) or 650 °C (b). (ii) After a first treatment with ethane dehydrogenation and a second treatment with CO_2 at 700 °C, when the ethane dehydrogenation was carried out at 600 °C (c) or 650 °C (d). (iii) After ethane ODH with CO_2 at 600 °C (e) or 650 °C (f). Red line corresponds to Cr^{3+} (main peak and two multiplet splitting peaks at higher BE); and blue line corresponds to Cr^{6+}.

Next, XPS studies were done by exposing the fresh sample to catalytic dehydrogenation (CD) conditions in an ethane/N_2 flow and stopping the reaction at two different temperatures, 600 and 650 °C, after 2 h of reaction (details in experimental section). In both cases Cr^{3+} were only observed in the XPS spectra (Fig. 7a), concluding this as the active specie under CD conditions. While Cr^{2+} with BE 575.5 eV was not detected in any case, their existence cannot be completely discarded, since it could exist bellow the limit of detection. Interestingly, when submitting both reduced samples to a flow of CO_2 and increasing the temperature up to 700 °C, Cr^{3+} is reoxidized to Cr^{6+}. The reoxidation take place in a higher

extension in the sample previously reduced in ethane/N_2 at 600 °C (showing ~ 35 % of Cr^{6+}) than in the one reduced at higher temperature, i.e., 650 °C (with ~ 16 % of Cr^{6+}) (Fig. 7, spectra c and d, respectively; and Table 1).

The different reoxidation pattern may indicate different types of reduced chromium species, with different reoxidation properties [21,23,24,26–28,30,35]. Thus, some authors postulate a reduction to Cr^{2+} as being responsible of coke formation [27] while other possibility is sintering of reduced polymeric Cr^{3+} species into Cr_2O_3 aggregates. According to some authors Cr_2O_3 cannot be reoxidized by CO_2 [23], behaving less active than polymeric chromium species.

Complementary studies were done using time and temperature resolved in situ Raman. Thus, studies under catalytic dehydrogenation (CD) conditions shows after 30 min of reaction at 600 °C the formation of a set of intense bands at 1350 cm^{-1} and 1600 cm^{-1}, named bands D and G [43] associated to carbon species or coke, and bands at 303, 344, 551 and 608 cm^{-1}, due to Cr_2O_3 [21,27], while the original band at 860 cm^{-1} due to CrO_3 is lost, pointing to Cr^{6+} reduction and partial sintering of Cr^{3+} species into Cr_2O_3 under reaction conditions (Fig. 8a). After 180 min of reaction at 600 °C, the bands at 303, 344, 551 and 608 cm^{-1}, while still present, are less detected (Fig. 8a).

Meanwhile, at 650 °C, while Cr_2O_3 and carbon are visible at 30 min of reaction, the former bands disappear completely after 180 min, remaining those of carbon only (Fig. 8b). The absence of bands due to Cr species in the Raman spectra can be explained, in line with the XPS data (Table 1), by a higher fraction of carbon species covering the catalyst surface, and inhibiting the detection of chromium species. Notice that Raman is a surface sensitive technique. According to these results, the lower catalytic activity at 650 °C vs 600 °C under CD conditions (see Fig. S1) can be explained by a higher carbon coverage of coke like species at the higher temperature (i.e., 650 °C), as discussed previously.

Next, XPS and Raman studies under ODH conditions, in the presence of CO_2, were done using an ethane/N_2/CO_2 flow and stopping the reaction at 600 or 650 °C. In the XPS study, after 2 h reaction (details in experimental section) at 600 °C, Cr^{6+} (10 %) and Cr^{3+} are detected (Fig. 7e). The presence of Cr^{6+} indicate a redox cycle between Cr^{3+} and Cr^{6+} promoted by the presence of CO_2, being Cr^{6+} the active site in ODH mechanism, in line with other authors [20,21]. However, at 650 °C, only Cr^{3+} is detected in the XPS Cr 2p peak (Fig. 7f), making a ODH mechanism less favorable, in favor to a CD path.

Based on these results, the prevalence of different reaction mechanism can be proposed in the presence of CO_2, being dependent on the reaction temperature. Thus, in the low temperature range (600–625 °C), a ODH mechanism predominate being Cr^{6+}-Cr^{3+} redox pair the active site, while in the high temperature range (650–675 °C), a CD mechanism predominate, being Cr^{3+} active specie. Here, an important point to consider is that, while analogous Cr^{3+} species have been detected in the XPS spectra of the sample exposed to CD conditions (in the absence of CO_2) at 650 °C, and the one exposed to ODH (in the presence of CO_2) at the same reaction temperature, the higher activity of the last one, may indicate an additional effect of CO_2, either in inhibiting sintering of Cr^{3+} species by reducing their activity, or in promoting or shifting the equilibrium of C-H activation, or in reducing coke formation.

On one hand, TG and DSC analysis of used catalysts at 600, 650 and 675 °C (Fig. S2 and Table 1) shows a lower amount of coke when the catalysts are used in the ethane ODH with CO_2, independently of the reaction temperature, while coke formation increases when increasing the reaction temperature. In addition, in situ Raman studies (Fig. 9)

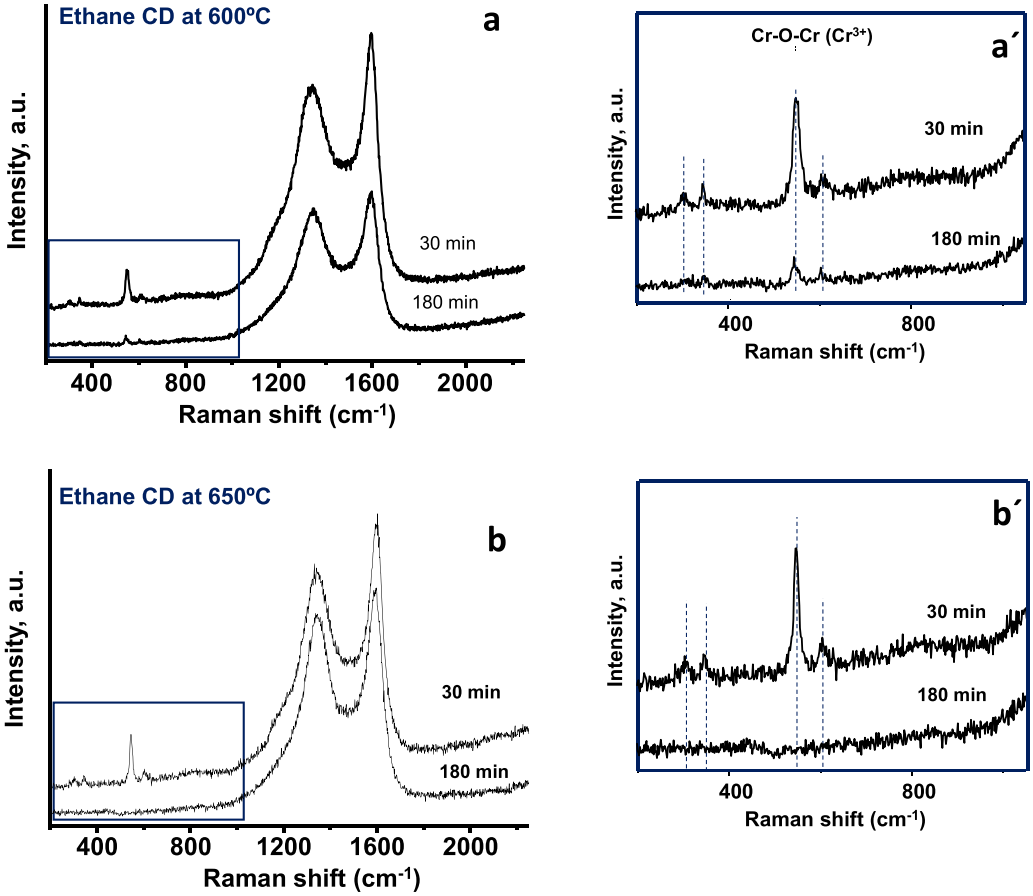

Fig. 8. Time and temperature resolved in situ Raman studies. Under catalytic dehydrogenation (CD) conditions at 600 °C (a) or 650 °C (b), using a flow of 30 mL min^{-1} ethane/N_2 (molar ratio of 12/88). Once achieved the target temperature, the reaction was kept for 30 min and 180 min. Spectra were collected by cooling down in helium flow to 200 °C. a´and b´are expanded Raman spectra in low frequency region.

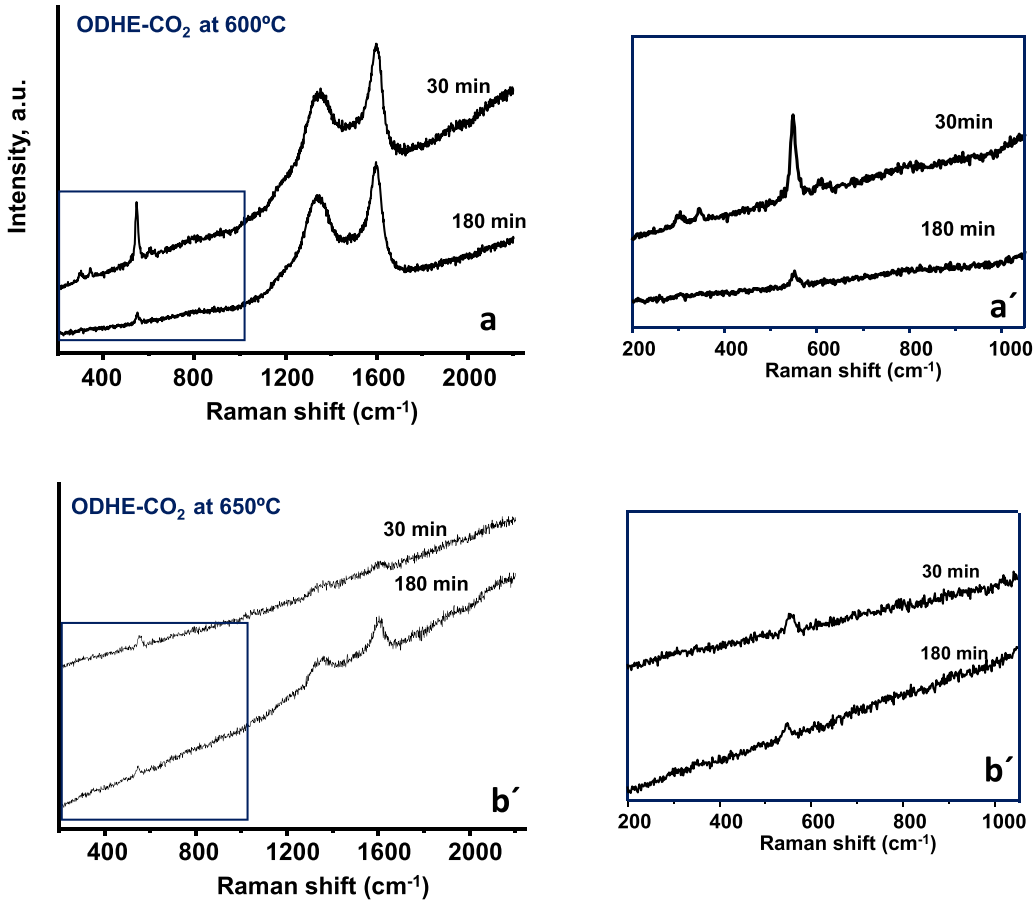

Fig. 9. Time resolved in situ Raman studies under oxidative dehydrogenation conditions, in the presence of CO_2, at 600 °C (a) or 650 °C (b), using a flow of 30 mL min^{-1} ethane/N_2 (molar ratio of 12/88). Once achieved the target temperature, the reaction was kept for 30 min and 180 min. Spectra were collected by cooling down in helium flow to 200 °C. a´and b´are expanded Raman spectra in low frequency region.

suggests that the presence of CO_2 slows down the formation of coke, in particular at 650 °C (Fig. 9b), as well as the formation of Cr_2O_3. This behavior contrast with that observed on the same catalyst in absence of CO_2 at the same temperature (see Fig. 8b).

Last, the activity and redox properties of Cr species have been studied by temperature-programmed TPR/TPO experiments done in the presence of ethane and CO_2, respectively. TPR studies in a flow of ethane at increasing temperature up to 600 °C (Fig. 10a), shows H_2 (m/Z = 2) evolution at 354 °C together with some amount of CO_2 (m/Z = 44) (Fig. 10a). At increasing temperatures, H_2O (m/Z = 18; at 506 ºC), CO_2 (m/Z = 44; at 558 °C) and finally CH_4 (m/Z = 15,16; at 586 °C) are also observed due to oxidation and cracking of surface adsorbed species. After reaching 600 °C in ethane/N_2 flow, the catalyst is cooled down to 25 °C and submitted to a second TPO process in a flow of 40 % CO_2/N_2 at increasing temperatures up to 700 °C. As shown in Fig. 10b, a peak due to CO formation is observed with an onset temperature of 431 °C and maxima at 682 °C together with a small peak of H_2 (m/Z = 2). CO may come from reoxidation of previously reduced Cr^{3+} species but can also be formed due to the reverse Boudouard reaction between coke and CO_2 [26]. In addition, H_2 may come from previous surface species which react with CO_2 resulting in CO and H_2 formation. In any case, while parallel reaction between surface species and CO_2 cannot be avoided, this experiment shows that the reoxidation of reduced surface Cr species is strongly limited taking place at high temperatures, in agreement with previous XPS data.

3.3. General remarks

The catalytic results presented here suggest a positive effect on ethane conversion with the presence of CO_2 in the feed specifically when the temperature is 650 or 675 °C and at time on streams higher than 100 min (Figs. S1a and S1b, Supplementary information). A similar conclusion can be proposed in the case of the yield of ethylene (Fig. S1c and S1d, Supplementary information).

These results are quite unexpected and actually differ from the ones found in the literature, in which the presence of CO_2 always enhances the catalytic activity in ethane ODH reactions with chromium oxides [21,24,26,27,30,35,44–46]. The same can be said when other oxides are used [47–49]. The conversion curves on Fig. 1a indicate that the ethane conversion is already stabilized at 600 and 625 °C for the ODHE-CO_2 experiments, while the ethane catalytic dehydrogenation, CD experiments (Fig. 1c), are still under deactivation effects at these temperatures. Based on the fact that the deactivation rate kept increasing at higher temperatures, we can assume that, when stable, the final ethane conversion at 600 and 625 °C for the CD experiments would be higher than the values found at 650 and 675 °C. That means the conversion of ethane for the CD experiments at 600 and 625 °C would still be higher than the ethane conversion for the ODH experiments, even on a longer experiment (see Figs. 1a and c).

Moreover, if we compare with the literature, ethane conversion at 30 min [46], or in the best of the cases below 300 min, ethylene yields of ca. 40 % at 650 °C are reported [45]. In addition, upon close inspection, the major difference found is that these studies used a CO_2:C_2H_6 feed ratio of 5:1, while we used a 2:1 ratio. It is possible that at high CO_2 concentrations, catalyst reoxidation is likely to occur even at lower temperatures. Indeed, in this work we found that CO_2 participates in limiting the formation of coke and avoiding the sintering of Cr^{3+} species, Thus, we can assume that both effects can be tuned depending on the

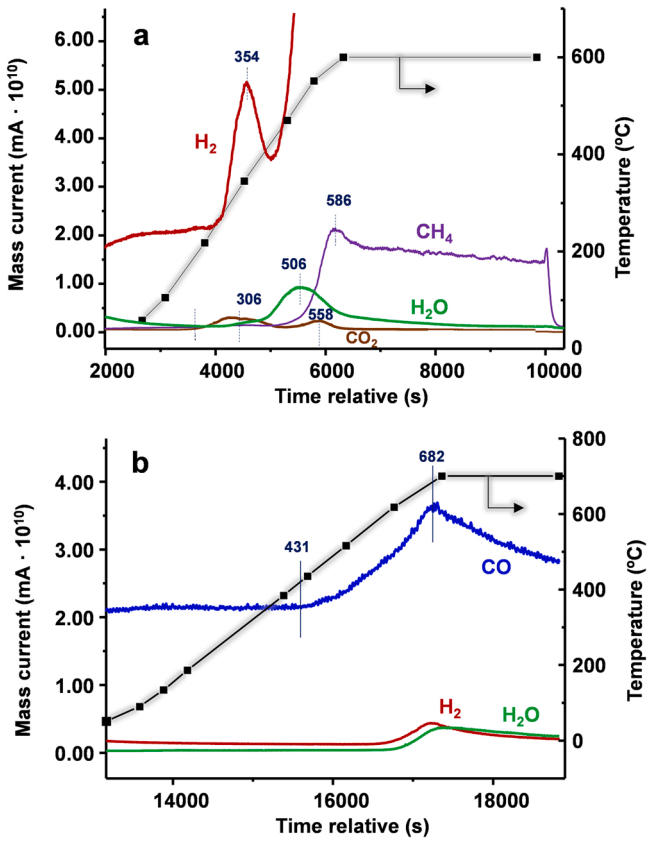

Fig. 10. Mass profile acquired during the temperature-programmed catalyst reduction with ethane, TPR-C_2H_6 (a) for sample 8CrAl; and the temperature-programmed catalyst re-oxidation with CO_2, TPO-CO_2 (b). Experimental conditions in text.

concentration of CO_2 in the reaction mixture.

Next, in order to verify the different reactions and pathways a careful analysis of the ratio of H_2, CO_2, CO and CH_4 in relation to ethylene was performed in this work. The conversions of ethane and CO_2 and yields of ethylene and CO for the ODH experiments are presented on Fig. 2. The conversion of ethane in relation to CO_2 (X_{C2H6}/X_{CO2}) remained close to 2 during the experiments. Since the ethane/CO_2 ratio in the feed gas is 1:2, the mole ratio (N_{C2H6}/N_{CO2}, mol/mol) should be equal to 1.

After calculation, the values closest to 1 were found for the experiment at 675 °C (1.02 and 0.99, time on stream of ca. 0 and 250 min, respectively), while the furthest were found for the experiment at 625 °C (1.12 and 1.22, time on stream of ca. 0 and 250 min, respectively). Accordingly, these results suggest that ODH reaction is the main reaction occurring. The yield curves of ethylene and CO are very similar. However, strong differences are observed depending on the reaction temperature. At a time of stream of c.a. 250 min, the yield of ethylene at 600 and 625 °C are practically the same, as are the yield values for CO. A similar trend is observed for the experiments carried out at 650 and 675 °C. Based on these results, it can be concluded that changes in the characteristics of used catalysts depended on the reaction temperature and are also likely related to the CO_2 concentration used in the experiments. These results confirm that, in addition to ODHE-CO_2, there are other reactions involved, such as dry reforming or the Boudouard reaction, which modify the ethylene/CO and H_2/CO ratios, depending on the reaction temperature.

In addition to the catalytic studies, a detailed analysis of the nature of the chromium active species and its dependence on the reaction conditions was done based on in situ spectroscopic studies. Thus, under CD conditions (in absence of CO_2), XPS data shows the existence of only Cr^{3+} species, behaving these as active sites (Fig. 11). In addition, Raman studies evidence the formation of coke (Fig. 8), being promoted at increasing temperatures, resulting in catalyst deactivation.

In ODH conditions (in the presence of CO_2), different chromium species are observed depending on reaction temperature (Fig. 12). Thus, it is shown that at low temperature (600–625 °C), CO_2 promote the re-

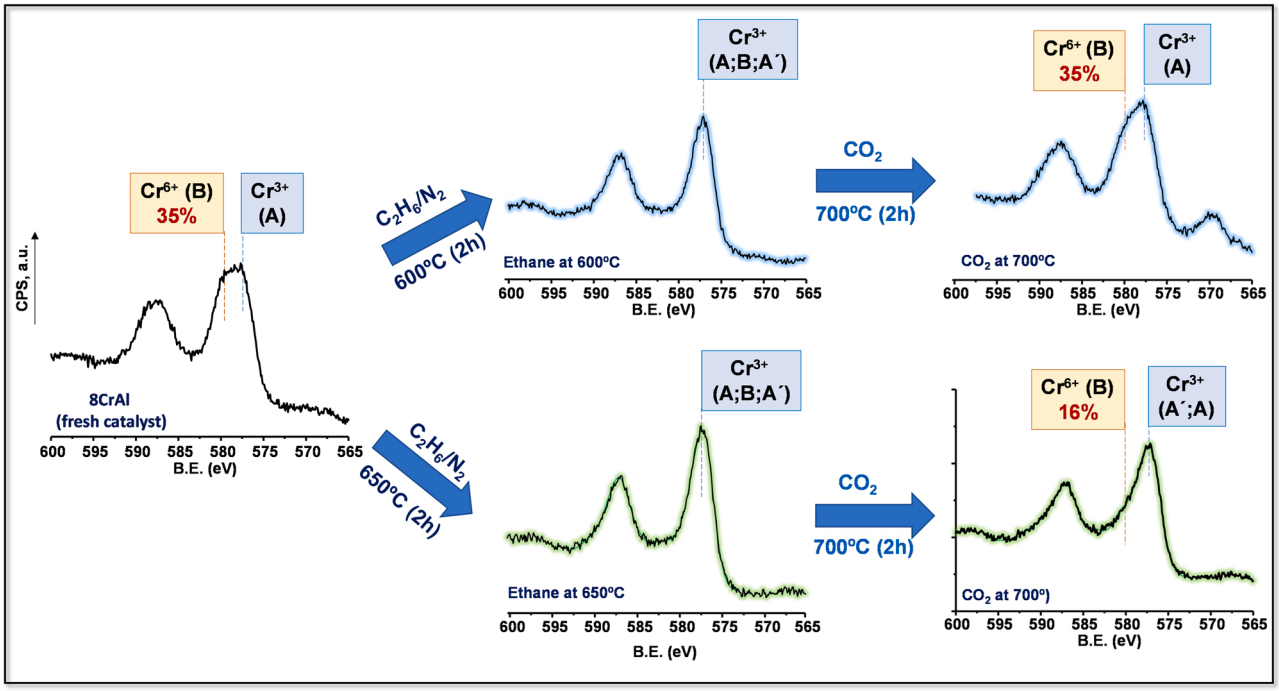

Fig. 11. General diagram of XPS spectra of Cr species under controlled reaction conditions. Left: original sample containing Cr^{3+} (labeled as A) and Cr^{6+} (labeled as B). Reduction of Cr^{6+}. Middle: reduction in ethane flow at 600 and 650 °C resulting in a reduction of Cr^{6+}(B) in Cr^{3+} (A). Right: reoxidation of Cr^{3+}(A) in CO_2 flow at 700 °C. Cr^{3+} is reoxidized to Cr^{6+} in a more extension in the sample previously reduced in ethane/N_2 at 600 °C than in the one reduced at higher temperature, i.e., 650 °C.

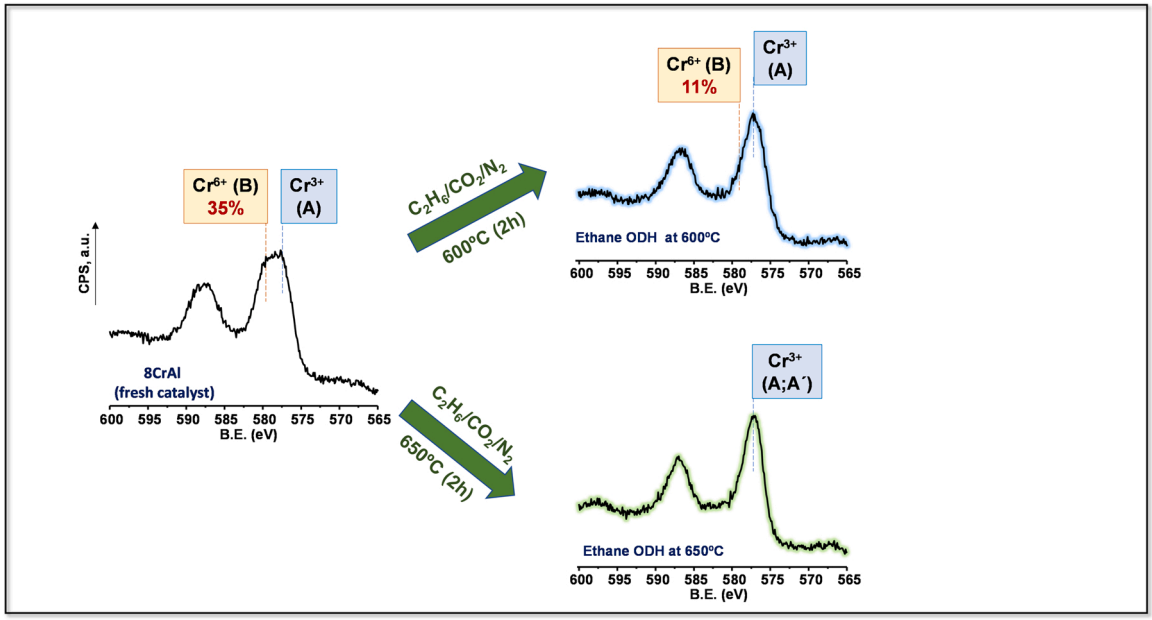

Fig. 12. General diagram of XPS spectra of Cr species identified under ODH-CO_2. Under these conditions, the reoxidation of Cr^{3+} to Cr^{6+} only takes place at 600 °C, and not at 650 °C.

oxidation of Cr^{3+} to Cr^{6+}, supporting a redox mechanism, where Cr^{6+} behaves as active specie, in line with previous studies in the literature. However, at increasing reaction temperature (650–675 °C), even in the presence of CO_2, only reduced Cr species (i.e., Cr^{3+}) are observed, whereas based on Raman studies, the role of CO_2 is in retarding coke formation and inhibiting the sintering of Cr^{3+} to Cr_2O_3. (Fig. 9b). Both features explain the higher catalytic performance obtained in the presence of CO_2 in the 650–675 °C temperature interval compared to those observed in the absence of CO_2 at similar temperatures.

4. Conclusions

In summary, the oxidative dehydrogenation of ethane in the presence and absence of CO_2 was studied on Al_2O_3-supported chromium oxide catalysts in the temperature range of 600–675 °C. The increase in the reaction temperature led to an increase in ethane conversion and ethylene selectivity for the ODH-CO_2 experiments.

In contrast to these experiments, in the absence of CO_2, the ethylene yield did not improve. Thus, after 4 h of experiment, the ethylene yield at 600 °C in the absence of CO_2 was higher than the experiment performed at 675 °C. This was due to a severe decay of catalytic activity. While this decay is observed in all experiments, the presence of CO_2 was able to mitigate this effect. Meanwhile, in the presence of CO_2, secondary reactions, such as RWGS, dry reforming, cracking reaction or the Boudouard reaction appears, as revealed by a modification of the CO/ethylene, H_2/ethylene and H_2/CO molar ratios.

In parallel, the nature of chromium species under reaction relevant conditions was also studied in this work using in situ spectroscopic studies. XPS analyses revealed the presence of Cr^{6+} and Cr^{3+} at the surface of fresh catalysts. In situ studies showed that, when the catalyst was reduced in the absence of CO_2, only Cr^{3+} species were present. This was corroborated by the in-situ Raman analysis, which showed a complete disappearance of bands related to Cr^{6+} after reduction in the absence of CO_2. The latter addition of CO_2 was able to re-oxidize some species of Cr^{3+} back to Cr^{6+}. The degree of reoxidation was dependent on the reduction temperature, as shown by the in situ XPS and the TPR-TPD analyses. This fact suggests the existence of different types of reduced Cr^{3+} species, capable of influencing the catalytic activity.

The influence of reaction temperature on the role of CO_2 was also studied, observing changes in the of role of CO_2 depending on the reaction temperature. At lower temperatures (600–625 °C), CO_2 promotes the re-oxidation of Cr^{3+} to Cr^{6+}. In this case, a redox mechanism was observed. On the other hand, at higher temperatures (650–675 °C), the reactions occur predominately via a catalytic dehydrogenation mechanism, as CO_2 is no longer capable of re-oxidizing Cr^{3+} to Cr^{6+}. Moreover, CO_2 favors partial elimination of coke, specifically at higher temperatures. This means that, even though ethylene yield is higher when compared to the lower-temperature experiments, it is no longer being generated by the ODH reaction, but via the CD reaction.

CRediT authorship contribution statement

G. do N. Franceschini: Investigation, Formal analysis, Writing - review & editing. **P. Concepción**: Methodology, Investigation, Formal analysis, Writing, Project Administration. **M. Schwaab**: Conceptualization, Supervision, Writing - review & editing. **M. do C. Rangel**: Methodology, Investigation, Formal analysis, Writing. **J. Martínez-Triguero**: Investigation, Formal analysis, Writing - review & editing. **J. M. López Nieto**: Conceptualization, Supervision, Project Administration, Writing - review & editing.

Declaration of Competing Interest

The authors declare that they have no known competing financial interests or personal relationships that could have appeared to influence the work reported in this paper.

Data availability

Data will be made available on request.

Acknowledgments

The authors would like to acknowledge the Ministerio de Ciencia e Innovación of Spain (projects PID2021–126235OB-C31, TED2021–130756B-C32 and the Generalitat Valenciana (project MFA/2022/016) for the financial support. The authors also acknowledge Coordenação de Aperfeiçoamento de Pessoal de Nivel Superior – Brasil

(CAPES/Print, UFRGS 2020) for the scholarship to G. do N. Franceschini.

Appendix A. Supporting information

Supplementary data associated with this article can be found in the online version at doi:10.1016/j.apcata.2023.119260.

References

[1] A.S.B. Naqyah, A. Al-Rabiah, Development and intensification of the ethylene process utilizing a catalytic membrane reactor, ACS Omega 7 (2022) 28445–28458.

[2] S.M.M. Sadrameli, Thermal/catalytic cracking of hydrocarbons for the production of olefins: a state-of-the-art review I: thermal cracking review, Fuel 173 (2015) 102–115.

[3] R.B. Dudek, F. Li, Selective hydrogen combustion as an effective approach for intensified chemical production via the chemical looping strategy, Fuel Process. Technol. 218 (2021), 106827.

[4] B. Subramaniam, R.K. Helling, Cl.J. Bode, Quantitative sustainability analysis: a powerful tool to develop resource-efficient catalytic technologies, ACS Sustain. Chem. Eng. 4 (2016) 5859–5865.

[5] I. Amghizar, L.A. Vandewalle, K.M. Van Geem, G.B. Marin, New trends in olefin production, Engineering 3 (2017) 171–178.

[6] S. Zafarnak, A. Bakhtyari, H. Taghvaei, M.R. Rahimpour, A. Iulianelli, Conversion of ethane to ethylene and hydrogen by utilizing carbon dioxide: screening catalysts, Int. J. Hydrog. Energy 46 (2021) 19717–19730.

[7] L. Tao, T.S. Choksi, W. Liu, J. Pérez-Ramírez, Synthesizing high-volume chemicals from CO_2 without direct H_2 input, ChemSusChem 13 (2020) 6066–6089.

[8] S.A. Chernyak, M. Corda, J.-P. Dath, V.V. Ordomsky, A.Y. Khodakov, Light olefin synthesis from a diversity of renewable and fossil feedstocks: state-of the-art and outlook, Chem. Soc. Rev. 51 (2022) (7994-804).

[9] J.T. Grant, J.M. Venegas, W.P. McDermott, I. Hermans, Aerobic oxidations of light alkanes over solid metal oxide catalysts, Chem. Rev. 118 (2018) 2769–2815.

[10] S. Najari, S. Saeidi, P. Concepcion, D.D. Dionysiou, S.K. Bhargava, A.F. Lee, K. Wilson, Oxidative dehydrogenation of ethane: catalytic and mechanistic aspects and future trends, Chem. Soc. Rev. 50 (2021) 4564–4604.

[11] A.M. Gaffney, J.W. Sims, V.J. Martin, N.V. Duprez, K.J. Louthan, K.L. Roberts, Evaluation and analysis of ethylene production using oxidative dehydrogenation, Catal. Today 369 (2021) 203–209.

[12] G. Li, C. Liu, X. Cui, Y. Yang, F. Shi, Oxidative dehydrogenation of light alkanes with carbon dioxide, Green Chem. 23 (2021) 689–707.

[13] Ya Gambo, S. Adamu, G. Tanimu, I.M. Abdullahi, A. Lucky, M.S. Ba-Shammakh, M. M. Hossain, CO_2-mediated oxidative dehydrogenation of light alkanes to olefins: advances and perspectives in catalyst design and process improvement, Appl. Catal. A: Gen. 623 (2021), 118273.

[14] S.T. Rahman, J.-R. Choi, J.-H. Lee, S.-J. Park, The role of CO_2 as a mild oxidant in oxidation and dehydrogenation over catalysts: A review, Catalysts 10 (2020) 1075.

[15] W. Sh. Raseale, K. Marquart, G. Jeske, M. Prieto, N. Claeys, Fischer, Supported FexNiy catalysts for the co-activation of CO2 and small alkanes, Faraday Discuss. 229 (2021) 208–231.

[16] A.N. Biswas, Zh Xie, J.G. Chen, Can CO_2-assisted alkane dehydrogenation lead to negative CO_2 emissions? Joule 6 (2022) 269–273.

[17] K. Baamran, Sh Lawson, A.A. Rownaghi, F. Rezaei, Process evaluation and kinetic analysis of 3D-printed monoliths comprised of CaO and Cr/H-ZSM-5 in combined CO_2 capture-C_2H_6 oxidative dehydrogenation to C_2H_4, Chem. Eng. J. 435 (2022), 134706.

[18] W. Gong, T. Wang, L. Wang, X. He, Y. Yao, S.T. Tjeng, D. Ding, M. Fan, High-performance of CrOx/HZSM-5 catalyst on non-oxidative dehydrogenation of C_2H_6 to C_2H_4: effect of supporting materials and associated mechanism, Fuel Proc. Technol. 233 (2022), 107294.

[19] P. Liu, L. Zhang, M. Li, N. Sun, W. Wei, Recent progress in Cr-based catalysts for oxidative dehydrogenation of light alkanes by employing CO_2 as a soft oxidant, Clean Energy 5 (2021) 623–626.

[20] A.S. Al-Awadi, S.M. Al-Zahrani, A.M. El-Toni, A.E. Abasaeed, Dehydrogenation of ethane to ethylene by CO_2 over highly dispersed Cr on large-pore mesoporous silica catalysts, Catalysts 10 (2020) 97.

[21] X. Li, S. Liu, H. Chen, S.Z. Luo, F. Jing, W. Chu, Improved catalytic performance of ethane dehydrogenation in the presence of CO_2 over Zr-promoted Cr/SiO_2, ACS Omega 4 (2019) 22562–22573.

[22] T.A. Bugrova, V.V. Dutov, V.A. Svetlichnyi, V. Cortés Corberán, G.V. Mamontov, Oxidative dehydrogenation of ethane with CO_2 over CrOx catalysts supported on Al_2O_3, ZrO_2, CeO_2 and $Ce_xZr_{1-x}O_2$, Catal. Today 333 (2019) 71–80.

[23] M. Numan, T. Kim, C. Jo, S.-E. Park, C.O.2 Assisted, Oxidative dehydrogenation of propane to propylene over fluidizable MoO_3/La_2O_3-γAl_2O_3 catalyst, J. CO_2 Util. 39 (2020), 101184.

[24] Z. Deng, X. Ge, W. Zhang, S. Luo, J. Shen, F. Jing, W. Chu, Oxidative dehydrogenation of ethane with carbon dioxide over silica molecular sieves supported chromium oxides: pore size effect, Chin. J. Chem. Eng. 34 (2020) 77–86.

[25] J. Liu, N. He, Z. Zhang, J. Yang, X. Jiang, Z. Zhang, J. Su, M. Shu, R. Si, G. Xiong, H. Xie, G. Vilé, Highly-dispersed zinc species on zeolites for the continuous and selective dehydrogenation of ethane with CO_2 as a soft oxidant, ACS Catal. 11 (2021) 2819–2830.

[26] T. Wan, F. Jin, X. Cheng, J. Gong, C. Wang, G. Wu, A. Liu, Influence of hydrophilicity and titanium species on activity and stability of Cr/MWW zeolite catalysts for dehydrogenation of ethane with CO_2, Appl. Catal. A-Gen. 637 (2022), 118542.

[27] Z. Xie, Y. Ren, J. Li, Z. Zhao, X. Fan, B. Liu, W. Song, L. Kong, X. Xiao, J. Liu, G. Jiang, Facile in situ synthesis of highly dispersed chromium oxide incorporated into mesoporous ZrO_2 for the dehydrogenation of propane with CO_2, J. Catal. 372 (2019) 206–216.

[28] E.V. Golubina, I.Yu Kaplin, A.V. Gorodnova, E.S. Lokteva, O.Ya Isaikina, K. I. Maslakov, Non-oxidative propane dehydrogenation on CrO_x-ZrO_2-SiO_{23} catalyst prepared by one-pot template-assisted method, Molecules 27 (2022) 6095.

[29] B.M. Weckhuysen, I.E. Wachs, Diffuse reflectance spectroscopy study of the thermal genesis and molecular structure of chromium-supported catalysts, J. Phys. Chem. 100 (1996) 14437–14442.

[30] J. Baek, H.J. Yun, D. Yun, Y. Choi, J. Yi, Preparation of highly dispersed chromium oxide catalysts supported on mesoporous silica for the oxidative dehydrogenation of propane using CO_2: insight into the nature of catalytically active chromium sites, ACS Catal. 2 (2012) 1893–1903.

[31] M.N.Z. Myint, B. Yan, J. Wan, S. Zhao, J.G. Chen, Reforming and oxidative dehydrogenation of ethane with CO_2 as a soft oxidant over bimetallic catalysts, J. Catal. 343 (2016) 168–177.

[32] F. Hu, X. Wu, Y. Wang, X. Lai, Ultrathin γ-Al_2O_3 nanofibers with large specific surface area and their enhanced thermal stability by Si-doping, RSC Adv. 5 (2015) 54053–54058.

[33] Y. Cheng, L. Zhou, J. Xu, C. Miao, W. Hua, Y. Yue, Z. Gao, Chromium-based catalysts for ethane dehydrogenation: effect of SBA-15 support, Microp. Mesop, Mater 234 (2016) 370–376.

[34] J.F.S. de Oliveira, D.P. Volanti, J.M.C. Bueno, A.P. Ferreira, Effect of CO_2 in the oxidative dehydrogenation reaction of propane over Cr/ZrO_2 catalysts, Appl. Catal. A Gen. 558 (2018) 55–66.

[35] A.S. Al-Awadi, A.M. El-Toni, S.M. Al-Zahrani, A.E. Abasaeed, M. Alhoshan, A. Khan, J.P. Labis, A. Al-Fatesh, Role of TiO2 nanoparticle modification of Cr/MCM41 catalyst to enhance Cr support interaction for oxidative dehydrogenation of ethane with carbon dioxide, Appl. Catal. A Gen. 584 (2019), 117114.

[36] A. Węgrzyniak, S. Jarczewski, A. Węgrzynowicz, B. Michorczyk, P. Kuśtrowski, P. Michorczyk, Catalytic behavior of chromium oxide supported on nanocasting-prepared mesoporous alumina in dehydrogenation of propane, Nanomater 7 (2017) 249.

[37] J.M. Kanervo, A.O.I. Krause, Characterisation of supported chromium oxide catalysts by kinetic analysis of H_2-TPR data, J. Catal. 207 (2002) 57–65.

[38] Y. Ohishi, T. Kawabata, T. Shishido, K. Takaki, Q. Zhang, Y. Wang, K. Takehira, Dehydrogenation of ethylbenzene with CO_2 over Cr-MCM-41 catalyst, J. Mol. Catal. A Chem. 230 (2005) 49–58.

[39] B.M. Weckhuysen, R.A. Schoonheydt, J.M. Jehng, I.E. Wachs, S.J. Cho, R. Ryoo, S. Kijlstra, E. Poels, Combined DRS–RS–EXAFS–XANES–TPR study of supported chromium catalysts, J. Chem. Soc. Faraday Trans. 91 (1995) 3245–3253.

[40] G. Neri, A. Pistone, S. De Rossi, E. Rombi, C. Milone, S. Galvagno, Ca-doped chromium oxide catalysts supported on alumina for the oxidative dehydrogenation of isobutane, Appl. Catal. A Gen. 260 (2004) 75–86.

[41] M.C. Biesinger, C. Brown, J.R. Mycroft, R.D. Davidson, N.S. McIntyre, X-ray photoelectron spectroscopy studies of chromium compounds, Surf. Interface Anal. 36 (2004) 1550–1563.

[42] M.C. Biesinger, B.P. Payne, A.P. Grosvenor, L.W.M. Lau, A.R. Gerson, Appl. Surf. Sci. 257 (2011) 2717–2730 (R. St. C. Smart).

[43] L. Li, R. Tan, S. Luo, C. Jiang, F. Jing, Controlled reaction depth by metal (M=Fe, Ni, Mn and Ti) doped ceria in selective oxidation of ethane with carbon dioxide, Appl. Catal. A Gen. 635 (2022), 118565.

[44] S. Xu, K.-F. Zhang, Y.-K. Ma, A.-P. Jia, J. Chen, M.-F. Luo, Y. Wang, J.-Q. Lu, Catalytic oxidation of dichloromethane over CrFeO mixed oxides: improved activity and stability by sulfuric acid treatment, Appl. Catal. A Gen. 636 (2022), 118573.

[45] F. Rahmani, M. Haghighi, One-pot hydrothermal synthesis of ZSM-5–CeO_2 composite as a support for Cr-based nanocatalysts: influence of ceria loading and process conditions on CO_2-enhanced dehydrogenation of ethane, RSC Adv. 6 (2016) 89551–89563.

[46] K. Nakagawa, M. Okamura, N. Ikenaga, T. Suzuki, T. Kobayashi, K. Nakagawa, M. Okamura, T. Suzuki, T. Kobayashi, T. Kobayashi, Dehydrogenation of ethane over gallium oxide in the presence of carbon dioxide, Chem. Commun. 3 (1998) 1025–1026.

[47] Q. Xie, C. Miao, W. Hua, Y. Yue, Z. Gao, Ga-doped MgAl2O4 spinel as an efficient catalyst for ethane dehydrogenation to ethylene assisted by CO_2, Ind. Eng. Chem. Res. 60 (2021) 11707–11714.

[48] Q. Xie, C. Miao, T. Lei, W. Hua, Y. Yue, Z. Gao, Dehydrogenation of ethane assisted by CO_2 over Y-doped ceria supported Au catalysts, React. Kinet. Mech. Catal. 132 (2021) 417–429.

[49] T.N. Phan, H.-S. Kim, D.-H. Kim, C.H. Ko, Mesoporous titania as a support of gallium-based catalysts for enhanced ethane dehydrogenation performance, Catal. Lett. 151 (2021) 2748–2761.